SCIENCE CHINA
Earth Sciences

• RESEARCH PAPER •

doi: 10.1007/s11430-011-4219-9

Interactions between hotspots and the Southwest Indian Ridge during the last 90 Ma: Implications on the formation of oceanic plateaus and intra-plate seamounts

ZHANG Tao[1,2,3,4*], LIN Jian[5] & GAO JinYao[3,4]

[1] *Institute of Geodesy and Geophysics, Chinese Academy of Sciences, Wuhan 430077, China;*
[2] *Graduate University of Chinese Academy of Sciences, Beijing 100049, China;*
[3] *The Second Institute of Oceanography, State Oceanic Administrator, Hangzhou 310012, China;*
[4] *Key Laboratory of Submarine Geosciences, State Oceanic Administrator, Hangzhou 310012, China;*
[5] *Department of Geology and Geophysics, Woods Hole Oceanographic Institution, Woods Hole, MA 02543, USA*

Received January 13, 2010; accepted October 14, 2010

This study investigates the relationship between the hotspot-ridge interaction and the formation of oceanic plateaus and seamounts in the Southwest Indian Ocean. We first calculated the relative distance between the Southwest Indian Ridge (SWIR) and relevant hotspots on the basis of models of plate reconstruction, and then calculated the corresponding excess magmatic anomalies of the hotspots on the basis of residual bathymetry and Airy isostasy. The results reveal that the activities of the Marion hotspot can be divided into three main phases: interaction with the paleo-Rodrigues triple junction (73.6–68.5 Ma), interaction with the SWIR (68.5–42.7 Ma), and intra-plate volcanism (42.7–0 Ma). These three phases correspond to the formation of the eastern, central, and western parts of the Del Cano Rise, respectively. The magnitude and apparent periodicity of the magmatic volume flux of the Marion hotspot appear to be dominated by the hotspot-ridge distance. The periodicity of the Marion hotspot is about 25 Ma, which is much longer than that of the Hawaii and Iceland hotspots (about 15 Ma).

Southwest Indian Ocean, hotspot-ridge interaction, magmatic volume flux, oceanic plateaus, seamounts

Citation: Zhang T, Lin J, Gao J Y. Interactions between hotspots and the Southwest Indian Ridge during the last 90 Ma: Implications on the formation of oceanic plateaus and intra-plate seamounts. Sci China Earth Sci, 2011, 54, doi: 10.1007/s11430-011-4219-9

Numerous seamounts are generated at plate boundaries by the volcanic and tectonic activities of mid-ocean ridges and transform faults [1]. Correspondingly, hotspots are mainly observed as intra-plate volcanism [2]. With the interaction of mid-ocean ridges and hotspots, the intensity of hotspot activity is amplified, resulting in the formation of broad plateaus [3]. These plateaus and seamounts (or seamount chains) substantially reflect the intensity of magmatism and the tracks of hotspots [2, 4–7], and record the ages, locations and magmatic volume of seamounts created by hotspots. It would be useful to study the time variation and periodicity of the intensity of hotspot activity and the interaction of hotspots, mid-ocean ridges and transform faults [4, 5, 8, 9]. Radioactive dating of rocks can be adopted to determine directly the ages of seamounts, and the thickness of the oceanic crust (layer 2A to layer 3) can be regarded as a first-order measure of the mantle magmatic volume [10]. However, very few rock samples have been taken and there has been little determination of the crustal thickness from seismic velocity profiles of ocean bottom experiments. In many areas that have been little studied, the mentioned methods cannot be used to calculate hotspot tracks and

*Corresponding author (email: zhangtaosio@gmail.com)

magmatic flux. Other geophysical methods, such as calculating the crustal thickness from topography or gravity data and calculating the crustal age from magnetic anomalies and plate reconstructions, have become the primary means of investigation [6, 11].

Compared with the East Pacific Rise and Mid-Atlantic Ridge, the region of the Southwest Indian Ocean has been less studied. Recently, the ultra-slow and oblique spreading characteristics of the Southwest Indian Ridge (SWIR) have attracted increasing international attention [12]. In 2007, a Chinese ship discovered the first active hydrothermal vent in the SWIR [13]. The Southwest Indian Ocean then became the focus of deep-sea research for its significance both in terms of science and resources. In addition to the northeast-striking SWIR, the study area also encompasses the Marion, Crozet and Conrad (extinct) hotspots, the Madagascar Plateau, the Del Cano Rise, the Conrad Rise and other features, and numerous unnamed seamounts (Figure 1). The formation of these plateaus and seamounts had been considered closely related to the SWIR and hotspots [14–16]. Owing to the sparse data of large-scale magmatic flux and plateaus (seamounts) dating, there was no clear understanding of the time variation in the intensity of the Marion and Crozet hotspots, the origin of the Del Cano Rise and Madagascar Plateau, and the interaction between hotspots and the SWIR.

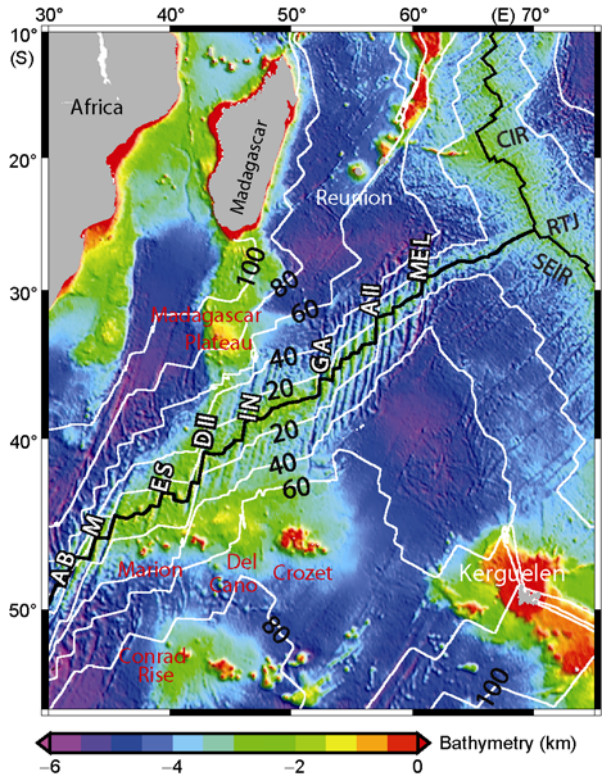

Figure 1 Bathymetric data of the study area based on satellite-derived data from Smith and Sandwell [17]. Hotspots and plateaus are indicated in red and the large transform faults in white. AB, Andrew Bain; M, Marion; ES, Eric Simpson; DII, Discovery II; IN, Indomed; GA, Gallieni; AII, Atlantis II; MEL, Melville. The intervals of the white contours of the crustal age are 20 Ma [18], and the ages are given in black. The black lines indicate the spreading center. CIR, Central Indian Ridge; SEIR, Southeast Indian Ridge; RTJ, Rodriguez Triple Junction.

In this study we first determined the relative positions of hotspots and the SWIR and the ages of plateaus and seamounts through plate reconstruction. Employing bathymetric anomalies and the Airy isostasy model, we then calculated the magmatic volume of hotspots to (1) determine the origin and evolution of plateaus and seamounts in the study area and their relationships with hotspots and the SWIR, (2) track the hotspots and analyze the temporal and spatial variations in hotspot intensity, and (3) discuss the interactions between hotspots, the SWIR and transform faults, and their effects on the geometric formation of the SWIR.

1 Geological background

The most significant topographic feature of the Southwest Indian Ocean has been shown to be numerous transform faults and the SWIR traversing the study area. The SWIR formed initially around 150 Ma ago [19], migrating rapidly from 80 Ma. Since 80 Ma, the ridge axis had migrated about 2500 km from DII to the Rodriguez Triple Junction (RTJ, 70°E) and sequentially formed GA, AII and MEL FZs (Fracture Zones) and so on [19]. Currently, the AB transform fault, with a length of about 1000 km, separates the SWIR into eastern and western parts [19]. Previous geophysical and geochemical studies have shown that there is a decreasing trend of the magmatic flux from west to east between the AB transform fault and RTJ [20–22]. According to the geophysics (bathymetry, side scan, gravity, and magnetic), geometry (the length of ridge segments, oblique spreading angle, incidence of transform fault), geochemical and petrologic characteristics of the SWIR, the eastern part of the SWIR is separated into four super segments by the DII (42°E), GA (52°20′E) and MEL (60°45′E) FZs [23, 24]. The shallowest part from the AB to DII FZs corresponds to a negative residual mantle Bouguer gravity anomaly (RMBA). It has been shown that intensive magmatism has caused a thickened crust or higher mantle temperature. This area may be affected by the Marion hotspot [23–25]. From the east of DII transform fault to 49°30′E, the ridge axis deepens and the RMBA becomes more positive. Accordingly, Georgen et al. [25] inferred that the eastward propagation of the Marion hotspot effect is blocked by the DII transform fault. The crustal thickness from the GA to MEL FZs determined by seismic velocity profiles is rather thin [26]. The largest average axis depth is from the MEL transform fault to the RTJ, and the crustal thickness thins continuously (average thickness of 4–5 km) as shown by seismic velocity profiles [27, 28]. There are fewer transform faults and numerous sites of exposed serpentine peridotites, which are typical of ultra-slow spreading ridges.

On the African plate north of the SWIR, the areas with

the shallowest depth include the Mozambique Ridge, Madagascar Plateau, and the ridge bathymetry anomaly extending from the Madagascar Plateau to the SWIR. There is still some debate about the origin of the Madagascar Plateau. On the basis of DSDP (Deep Sea Drilling Project) drilling data recorded at sites 246 and 247 of Leg 25, Coffin et al. [15] considered the Madagascar Plateau as the continental crust, but neither hole at the sites totally penetrated the sediment layer. Seismic velocity profile data shows that the northern and southern parts of the Madagascar Plateau (with 31°S as the boundary) are more inclined to be considered as the oceanic crust and might have originated from Cretaceous hotspot activity, although there are differences in the crustal structures [29]. The ridge bathymetry anomaly from the Madagascar Plateau extending to the spreading center has been considered as the track of the Marion hotspot [25, 30]. There are numerous plateaus such as the Conrad Rise, Marion hotspot, Del Cano Rise and Crozet Plateau on the Antarctic plate south of the SWIR. The shallowest area of the Conrad Rise, which is south of the SWIR and conjugated to the Madagascar Plateau, is close to sea level, and there may be an extinct hotspot under its southeast seamount (48°E, 53°S) [31]. The Marion hotspot, Del Cano Rise and Crozet Plateau together constitute a hotspot swell with a diameter of more than 1000 km. Some researchers have considered them as a hotspot group. The Marion hotspot is one of several active hotspots of long geological history. At about 88 Ma, its magmatism created the Volcan de l'Androy lava pile on southern Madagascar and might have caused the breakup of Madagascar and India [32]. Coffin et al. suggested that the Del Cano Rise might have been created by the magmatism of the Marion hotspot [15]. Analyzing the depth-gravity admittance function of the Del Cano Rise, Goslin et al. [33] considered that this area approached local isostasy and was generated on a weaker lithosphere in the proximity of a spreading center. The Del Cano Rise is close to the Crozet Plateau, but both the isostasy analysis and seismic velocity profiles indicate a difference in their geological origins [34]. The Crozet Plateau is also currently active, but its origin and track are still a subject of considerable debate [31, 35, 36].

2 Residual bathymetry of the Southwest Indian Ocean

Bathymetry data are a visualization of the magmatism of hotspots and mid-ocean ridges. As the topography of seamounts and plateaus was modified by the effects of lithosphere subsidence, sediment filling, compaction and other factors, these influences were subtracted from the observation data in this study, and the residual bathymetry was obtained to reflect the magmatism at the time of crust formation.

2.1 Data and errors

The bathymetry data used in this study were the latest 1′×1′ satellite-derived data (Version 11.1) from Smith and Sandwell [17], and they are presented in Figure 1. With the addition of more depth sounding data, 75% of the data were within 24 km of a sounding point. In regions with complex topography, the data, being significantly more accurate than data of previous versions, were suitable for studying the SWIR and seamounts of great depth variations. Along the SWIR, the multi-beam data with 100 m×100 m grid spacing were compared with the Version 11.1 of depth data in this study (multi-beam data recorded by the Gallieni Cruise of French L′Atalante [20]) employing the accuracy evaluation methods of Smith and Sandwell [17]. The root mean square of the depth variation in the multi-beam coverage area was 4613 m, while the difference between satellite altimeter data and multi-beam data was only 198 m. This indicates that the confidence of the latest version of satellite-derived data might reach 96%.

We used the 2′×2′ oceanic crustal age data released recently by Muller et al. [18] as shown in Figure 2. In the study area, the new 2′×2′ model includes more ship track magnetic data and thus is better than the 6′×6′ crustal age model widely used previously. The error of the crustal age data for 58.9% of the entire study area was less than 2 Ma,

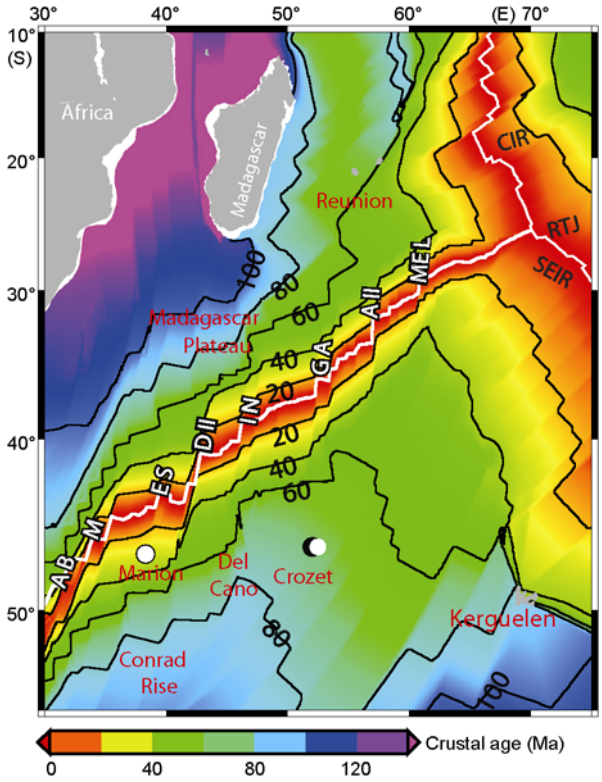

Figure 2 Crustal age model with contour intervals of 20 Ma [18]. Crustal ages are given in black font. Hotspot locations are indicated with white solid circles. Names of hotspots and plateaus are given in red font and large transform faults are given in white font.

while that for 93.7% of the entire area was less than 5 Ma. The areas with data errors greater than 5 Ma were mostly the transition area between ocean and land or the fracture zones, which had little effect on this research. The crustal ages of the Marion and Crozet hotspots are about 30 and 70 Ma, respectively, and that of the Conrad Rise is about 90 Ma.

We used 5′×5′ grid data provided by Divins [37] for the sediment thickness in this study, and they are presented in Figure 3. These data were compiled from the published sediment thickness isopach map, data from DSDP and ODP (Ocean Drilling Program), and data from the NGDC, IOC and GAPA projects. The average sediment thickness of the study area was 0.75 km. Except for areas adjacent to land, the sediment thickness was positively correlated to the crustal age, and the sediment was obviously thicker on the plateaus and hotspots. The sediment thickness around the Marion and Crozet hotspots was close to 1 km.

2.2 Methods

During the spreading to both sides, the lithosphere cools and becomes denser gradually, leading to the continuous subsidence of the lithosphere and sea floor. In the lithosphere subsidence equations, for both the half-space plate cooling models, the crustal age has been considered as a key variable [38–40]. Compared with other methods, the modified

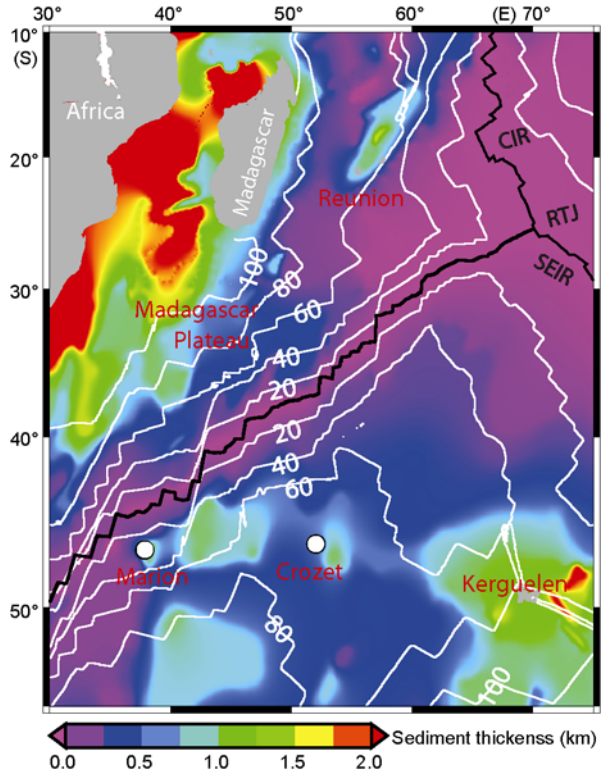

Figure 3 Sediment thicknesses isopach map [37]. Hotspot locations are indicated with white solid circles. Hotspots and plateaus are given in red font. Crustal age contours with intervals of 20 Ma are given.

equation (eq. (1)), proposed by Stein and Stein according to the correlation between heat flow data and depth data, is particularly useful and simple [40]. In addition, the theoretical values are more consistent with observations for older crusts. The modified equation was used in this study to calculate the residual bathymetry.

$$D=2600+365t^{1/2},\ t<20\ \text{Ma},$$
$$D=5651-2473\exp(-0.0278t),\ t\geqslant 20\ \text{Ma}, \quad (1)$$

where D is the subsidence value (m) and t is the crustal age (Ma).

The sediments have two effects on depth data. One is the filling and compaction of sediments resulting in a shallower sea floor depth and the other is the sediment load resulting in isostatic adjustment of the lithosphere, deepening the sediment basement. With the sediment thickness subtracted from the observed depth, the empirical formula (2) was used to calculate the lithosphere deformation caused by sediment loads. Crough [41] used DSDP data to derive a relationship between sediment thickness and correction values. The empirical formula (2) is a simple fit of this relationship (the mean square deviation between the raw data and the fitted data was about 0.06 km), being suitable for the area of sediment thickness less than 1.8 km [41].

$$S=0.22c+0.00014c^2-c, \quad (2)$$

where S is the correction value of sediment effects (m) and c is the sediment thickness (m). The residual bathymetry is

$$\text{RB}=B-D+S, \quad (3)$$

where RB is the residual bathymetry and B is the observation value.

2.3 Residual bathymetric anomalies

In the map of residual bathymetry (Figure 4), the huge swell of the Marion hotspot, Del Cano Rise and Crozet hotspot was the area having the most significant anomalies. As with other hotspots around the world, this swell with a spatial extent of about 1000 km originated from the supporting force of the upwelling hot mantle material and the excess magmatic crust by hotspots. With Marion-Del Cano-Crozet as the center, the southward and eastward parts of the swell had a spatial extent of no more than 300 km, while the part near the north and west of the SWIR had an extent of nearly 1000 km. This difference might result from the effect of the Marion and Crozet hotspots being amplified by the SWIR. The southern ends of the Madagascar Plateau and Conrad Rise were symmetrically distributed around the SWIR and had similar residual bathymetry. The ridge-shaped bathymetric anomaly extending from the Madagascar Plateau to the SWIR has been considered as the hotspot track [25, 30]. Along the triple-junction track, there was north-south symmetric uplift between the IN and AII FZs, which gener-

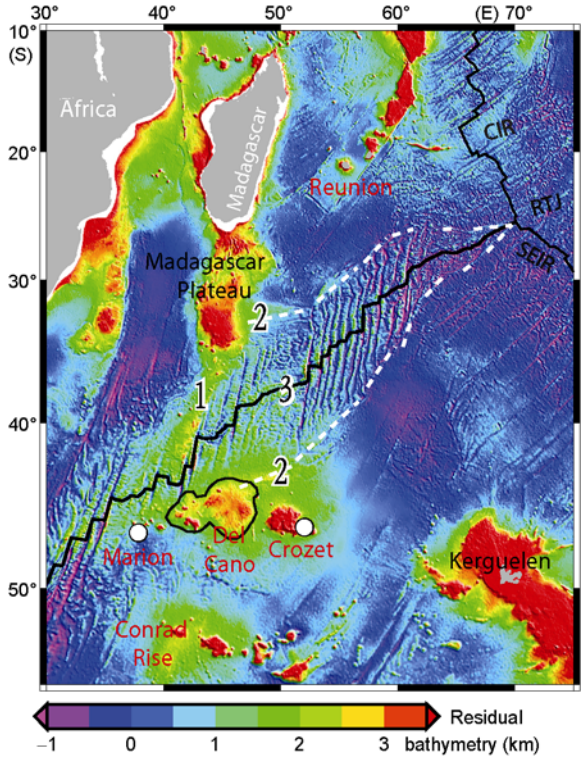

Figure 4 Calculated residual bathymetry of the Southwest Indian Ocean. Hotspot locations are indicated with solid white circles. The hotspots and plateaus are given in red font. The spreading center is indicated with black lines. The triple-junction tracks are indicated with white dashed lines. The Del Cano Rise is circled in black, and numbers represent the unnamed bathymetry anomalies discussed in this study. 1 indicates the ridge-shaped bathymetry anomaly extending from the Madagascar Plateau to the SWIR; 2 indicates the symmetric V-shaped topography along the triple-junction track from the IN to AII FZs; 3 indicates the topographic uplift from the IN to GA FZs.

ally showed a gradual contraction of a V-shaped bathymetry anomaly from west to east. Within the track of the triple junction, the ridge axis west of the GA transform fault was much shallow than that east of the GA transform fault. It is seen that the segment of the SWIR to the west of the GA transform fault was influenced not only by hotspots [25] but also had influenced since the formation of the GA transform fault. The bathymetry anomaly in the area of the active spreading ridge between the IN and GA FZs is also seen to have a contracted "V" shape from west to east. The anomaly might be influenced by the Crozet hotspot [42]. Similar to the slow spreading Mid-Atlantic Ridge, the ridge-transform inside corners were frequently distributed between GA and AII FZs and they are associated with significantly high topography. The high topography of the ridge-transform inside corners might originate from the footwall uplift of the detachment faults [43] rather than magmatism.

3 Plate reconstruction

On the basis of the Atlantic-Indian Ocean hotspots reference system provided by Muller et al. [31], a finite Euler pole was used for plate reconstruction (Figure 5) in this study. The study area includes the four large plates of Africa, Antarctica, Australia and the India-Mid-India basin, and the plate boundary data were taken from the Nuvel-1 model [44]. The geochemical and petrological data demonstrated clearly that the Marion hotspot was located on Madagascar Island [32] around 90 Ma and approached the spreading center gradually; therefore, 90 Ma was selected as the initiation time of reconstruction in this study.

As shown in Figure 5(a), the Marion hotspot was located on the eastern side of Madagascar Island at 90 Ma (i.e. the Volcan de l'Androy lava pile), which is consistent with previous geochemical evidence [32]. The Madagascar Plateau and Conrad Plateau with similar residual bathymetry then overlapped, while the triple junction was located to the east of the Madagascar Plateau and moved slowly toward the northeast. As the Marion hotspot was located on the northern Madagascar Plateau at 84 Ma (Figure 5(b)), the Conrad Plateau and Madagascar Plateau were almost separated, and the crust where the Conrad Rise was located had formed. Subsequently, as the African plate and the triple junction moved to the northeast, the paleo-RTJ approached the Marion hotspot gradually (Figure 5(c)). At 73.6 Ma (Figure 5(d)), the paleo-RTJ was only 160 km from the Marion hotspot, while the Crozet hotspot was located near southeastern India. The southern crust where the Crozet hotspot was located had formed by that time. From 73.6 to 68.5 Ma (Figure 5(d), (e)), the paleo-RTJ was closer to the Marion hotspot, and the eastern Del Cano Rise and southeastern Madagascar Plateau formed on both sides of the SWIR. From 68.5 to 58.5 Ma (Figure 5(e), (f)), the paleo-RTJ moved rapidly to the northeast, leading to the steady and stable generation of the IN, GA, and AII FZs. The speed of the paleo-RTJ propagation was 8 times the current spreading rate. Meanwhile, the Marion hotspot was close to or located on the spreading center, where strong magmatism created the middle of the Del Cano Rise. With the hotspot effect propagating along the SWIR, an east-pointing V-shaped plateau with length over 1000 km formed in the vicinity of the SWIR bounded by the IN, GA, and AII FZs. With the spreading of the SWIR, the plateau was split into a north-south symmetric topography anomaly along the triple-junction track (with the current location shown in Figure 4). At the same time, the Crozet hotspot reached the Antarctica plate across the Southeast Indian Ridge; however, there are no obvious topography anomalies on its track. At 50.3 Ma (Figure 5(g)), the Marion hotspot was close to or on the SWIR between the DII and IN FZs, and a symmetrical high topography anomaly formed on both sides of the SWIR. The northern side of the anomaly was the southern end of the Madagascar Plateau, and the southern side was the central area of the Del Cano Rise. From 42.7 to 35.5 Ma (Figure 5(h), (i)), the spreading center moved far from the Marion hotspot gradually, while the Marion hotspot was

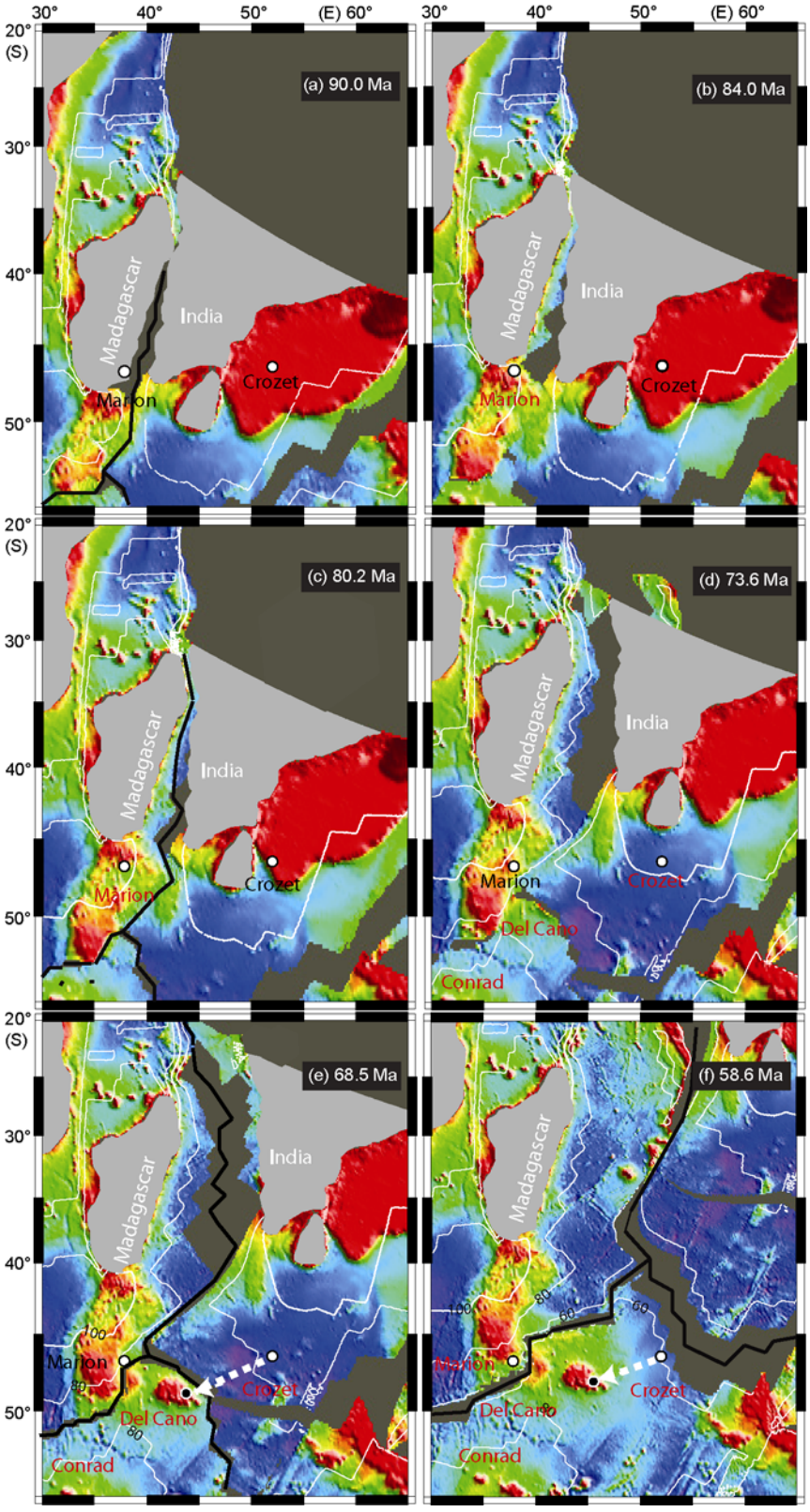
30°
40°
50°
(E) 60°
20°
(S)
30°
40°
50°
(a) 90.0 Ma
(b) 84.0 Ma
(c) 80.2 Ma
(d) 73.6 Ma
(e) 68.5 Ma
(f) 58.6 Ma
Madagascar
India
Marion
Crozet
Del Cano
Conrad
100
80
60

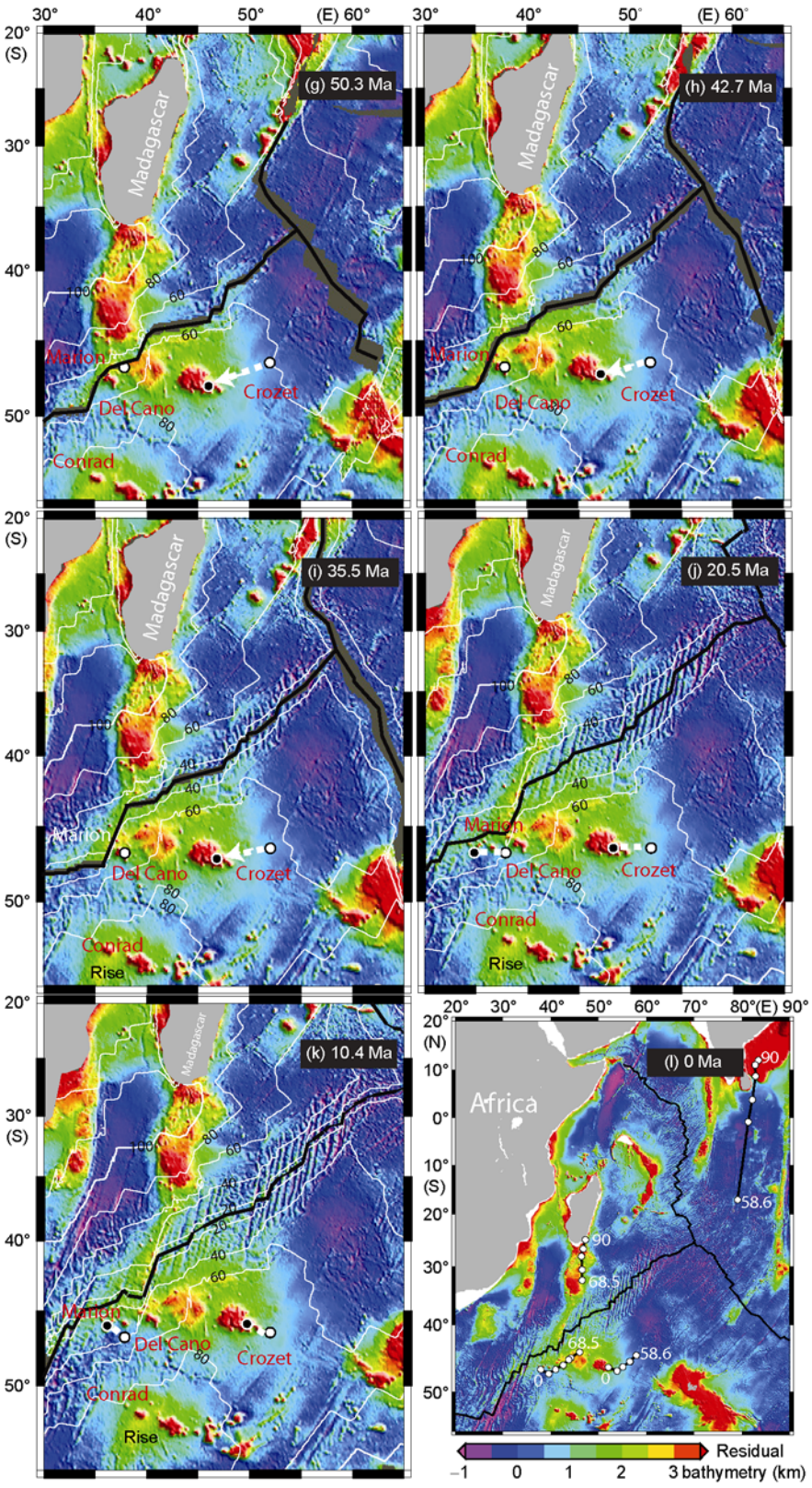

Figure 5 Plate reconstruction of the Southwest Indian Ocean based on the hotspot absolute reference system. In (a)–(k), the base map is the residual bathymetry map at the corresponding age. The crustal ages with intervals of 20 Ma are indicated with white contours and values are given in black. The paleo ridges are indicated with black lines. The Marion hotspot and Crozet hotspot are indicated with white solid circles. The current locations of the hotspots are indicated with solid black circles, and the historical and present locations are connected with white dotted lines; (l) shows the tracks of hotspots on the corresponding plates, where white solid circles correspond to hotspot locations at different ages. The origin-end ages are given in white font, and hotspot tracks are indicated with black lines.

located in the eastern crust of the AII transform fault and had a crustal age of 53 Ma, and formed the western part of the Del Cano Rise. Meanwhile, a ridge topography anomaly extending from the Madagascar Plateau to the SWIR formed on the western side of the transform fault. Because there was no corresponding topography anomaly on the southern side of the SWIR, it is inferred that this topography anomaly did not form on the SWIR. From 20.5 Ma to the present (Figure 5(j)–(l)), the African plate had a clear direction change relative to the Marion hotspot, moving eastward instead of the original nearly northern direction. At this time, the Marion hotspot had reached the current location of hotspot activity. In contrast with activity of the Marion hotspot, there was no obvious topography anomaly on the track of the Crozet hotspot during this whole process.

4 Estimation of magmatic flux

Compared with other methods, calculating the magmatic flux from bathymetry data is more visual and convenient. Thereby, it is widely used in magmatic flux studies on the Hawaiian hotspot of the Pacific as well as the Walvis and St. Helena hotspots of the south Atlantic [8, 9, 45]. If the Moho is considered as a compensation level and the local isostasy is assumed, the shape of the Moho and the crustal thickness could be calculated from the residual bathymetry. Because the lithosphere of mid-ocean ridges is very weak, the created seamounts in this area are mostly close to the local isostasy model. Therefore, the crustal thickness generated on the SWIR was calculated in this study according to the Airy isostasy model.

$$F_{\text{Airy}} = \left(1 + \frac{\rho_{\text{v}} - \rho_{\text{w}}}{\rho_{\text{m}} - \rho_{\text{v}}}\right) h + R, \tag{4}$$

where ρ_{v} is the density of the volcanic crust, ρ_{w} is the sea water density, and ρ_{m} is the mantle density, with values given as 2800, 1030 and 3300 kg/m^3, respectively. R is the interlayer between the reference level of the topography uplift and the "mountain root" and is given as 6 km, leading to a calculated crustal thickness of the Del Cano Rise consistent with that determined from seismic velocity profiles [34]. The calculated crustal thickness is shown in Figure 6.

According to the seamounts age provided by plate reconstruction, the crustal thickness was integrated at a corresponding age in this study, and the time variation of the magmatic flux of the Marion hotspot was obtained. The 6 km reference crustal thickness was subtracted from the magmatic anomaly to remove the effects of normal crust and hotspot swell (see section 5.1). From 80.2 to 42.7 Ma (Figure 5(c)–(h)), the Marion hotspot was very close to the triple junction and the SWIR, and its magmatic flux could be represented with continuous crust accretion. From 42.7 Ma to the present (Figure 5(h)–(l)), hotspots were mainly shown as the intra-plate volcanism rather than a continuous process. The magmatic flux was taken as the mean value of this period in this study. As shown in Figure 7(a), the hotspot effect was amplified as continuous intense magmatism when the SWIR was close to the Marion hotspot. The peak periods of two excess magmatic fluxes at about 74 and 50 Ma corresponded to two periods of the Marion hotspot: one when the hotspot was adjacent to the paleo-RTJ and one when the hotspot was on the SWIR. These were the periods of formation of the eastern and central parts of the current Del Cano Rise respectively. From 42.7 to 35.5 Ma, the effect of the Marion hotspot was mainly intra-plate volcanism. The mean value of this magmatic flux was obviously smaller than that in the interaction of the hotspot and the SWIR, and the maximum mean value only accounted for 1/6 or 1/5 of that at 74 and 50 Ma, respectively (Figure 7(a)). With the hotspot moving far away from the SWIR, its excess magmatic flux reduced further. The activity of the Marion hotspot decreasing with time was consistent with the conclusion of Georgen et al. [25]. However, the residual bathymetry (Figure 7(b)) on the hotspot track reveals that when the hotspot was far from the SWIR (about 30 Ma), the depth was shallower than that at 74 and 50 Ma. This indicates that the intra-plate magmatism of hotspots was more focused and tended to create shallow seamounts, while the effect of hotspots propagating along mid-ocean ridges tended to create a broad low-amplitude plateau as hotspots

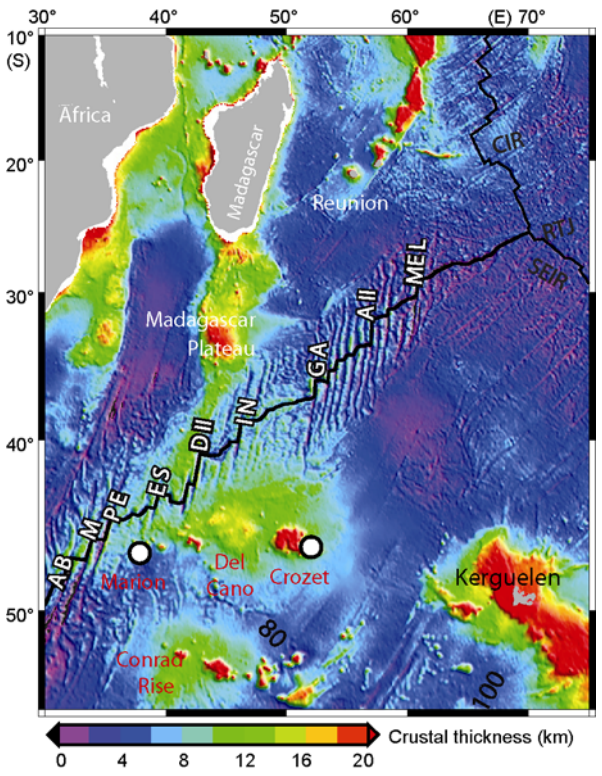

Figure 6 Calculated crustal thickness based on the Airy isostasy model. The locations of hotspots are indicated with white solid circles. The names of hotspots and plateaus are given in red. The main transform faults are given in white. The spreading center is indicated with black lines.

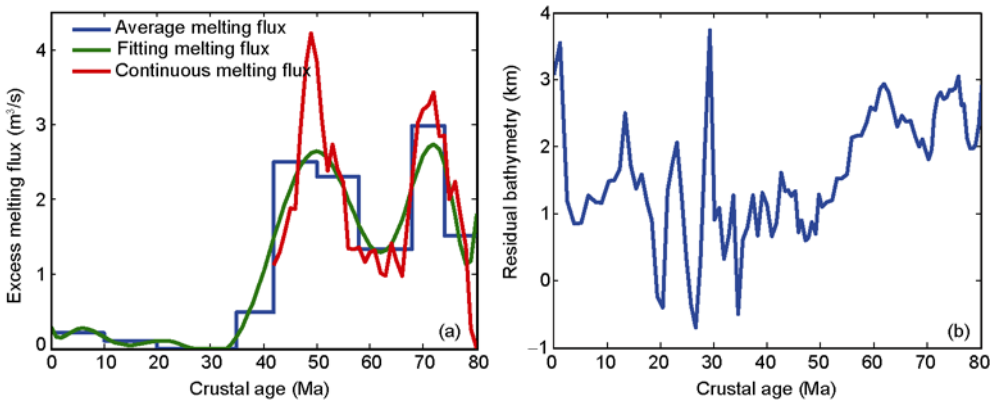

Figure 7 Time variation of the excess magmatic flux of the Marion hotspot. (a) Time variation of the excess magmatic flux of the Marion hotspot; (b) time variation of the residual bathymetry on the track of the Marion hotspot.

interacting with mid-ocean ridges.

5 Discussions

5.1 Model errors and their influences on the results

It is hypothesized that both plateaus and seamounts in the study area are consistent with the Airy isostasy model. During the intra-plate activity of hotspots, the lithosphere already had certain strength. Therefore, the effective elastic thickness of the lithosphere at the time of seamount formation should be considered in the calculation of the compensation level, and a regional compensation model rather than a local compensation model should be used to calculate the total magmatic volume. However, studies on Hawaiian seamounts indicated that different compensation models only changed the shape of the compensation level without influencing the volume of the total magmatic volume [8]. As the present study focused on the magmatic flux, the use of the Airy model does not significantly affect the results.

In the areas of hotspot activity, it is supposed that the hotspot swell with a range of up to several thousand kilometers originates from magmatism or the mantle support force. As shown in Figure 8, the former model used in calculating magmatic flux includes the hotspot swell, whereas the latter was required to eliminate the hotspot swell effect. Because studies on Hawaiian seamounts considered that the swell originates from mantle support [8], the swell effect was eliminated in calculating the magmatic flux in this study. Wessel systematically summarized the advantages and disadvantages of various methods of eliminating the hotspot swell effect [46]. The simple symmetry of the SWIR was used to eliminate the influence here. The symmetric topography between IN and AII FZs on the triple-junction track is due to the same plateau being generated by the hotspot effect along the SWIR. The symmetric topography is supposed to have consistent depth values. Because the northern part was not influenced by hotspot swell, the difference in depth between the southern and

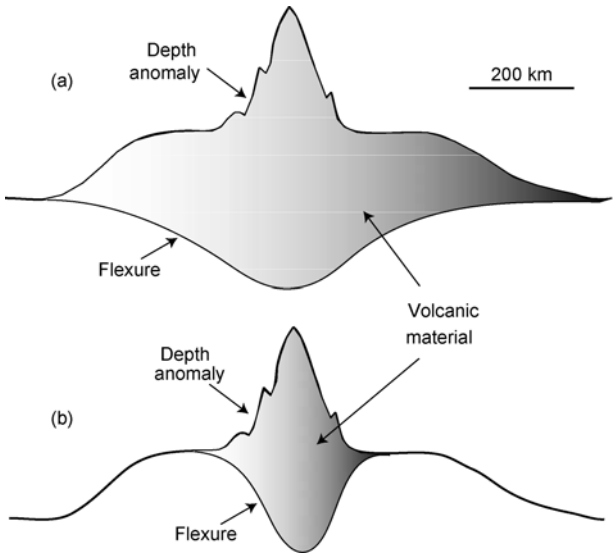

Figure 8 Schematic diagram of the hotspot swell model, modified from Vidal et al. [8]. (a) The magmatic flux with hotspot swell; (b) the magmatic flux without hotspot swell.

northern parts is the correction value of the swell. In addition, because the central area of the hotspot swell is broad with low amplitude changes, a constant correction value was adopted here.

The plate reconstruction data used in this study were based on the absolute reference frame of the Atlantic-Indian Ocean hotspots, while increasing recent evidence indicates that hotspots are not fixed on an absolute reference frame [47]. However, the velocity of hotspots was much lower than that of plates, and hotspots in the Southwest Indian Ocean mostly had similar tracks [47]. The movement of hotspots does not influence the key conclusions for the large-scale issues discussed in this study.

5.2 Ridge-shaped bathymetry anomaly to the south of the Madagascar Plateau

The ridge-shaped bathymetry anomaly extending from the

Madagascar Plateau to the SWIR has been considered as the track of the Marion hotspot when the hotspot crossed the ES-DII segment of the SWIR to reach their current locations along this bathymetry anomaly [25, 30]. The reconstruction in this study shows that the hotspot track was mostly located on the eastern side of DII and did not correspond to the ridge-shaped bathymetry anomaly. Meanwhile, no plateau formed as the hotspot crossed the segment between ES and DII FZs. Therefore, it is considered that this bathymetry anomaly may have been the result of the effect of the Marion hotspot, which was located on the eastern side of DII and penetrated the transform fault in this study. This model is similar to the seamount chain generated by the Discovery hotspot of the south Atlantic penetrating the Agulhas transform fault on the other side [48]. That is, owing to the age offset of the two sides, there would be a slope of certain angle at the bottom interface of the lithosphere from one side of the transform fault to the other, leading to the hotspot effect propagating from one side of the transform fault to the other. As a result, a seamount chain formed on the other side of the Agulhas transform fault [48].

5.3 Formation of the Del Cano Rise

The Del Cano Rise and its surrounding topographic anomalies are associated with all kinds of hotspots activities, including interaction with the triple junction, the SWIR and transform faults as well as intra-plate seamount activities. From 80 to 68.5 Ma, the eastern Del Cano Rise formed as a consequence of the paleo RTJ and the hotspot, the main part of the Del Cano Rise then formed owing to continuous interaction of the SWIR and the hotspot, and the western seamounts formed as intra-plate seamounts from 42.5 to 35 Ma. As the lithosphere of the triple junction and mid-ocean ridges were weak, they tend to have Airy local isostasy. Therefore, the main part of the Del Cano Rise was in a local isostasy state while the intra-plate seamounts were mainly in a regional isostasy state. This is consistent with the interpretations of the isostasy state of the Del Cano Rise and Crozet hotspot by Goslin et al. employing gravity analysis [29].

5.4 Temporal variation of the Marion hotspot magmatic anomaly

We compared the excess magmatic flux of the Marion hotspot and that of the Hawaii and Iceland hotspots in this study [4, 5], as shown in Figure 9(a). Except for the tremendous magmatic flux (about 55 m^3/s) generated by the Greenland-Iceland ridge close to the continental margin at 53 Ma, the fluxes of the Hawaii and Iceland hotspots were relatively consistent in terms of value and trend. Compared with the Hawaii and Iceland hotspots, the magmatic flux of the Marion hotspot has been much smaller since 40 Ma. In the two peak periods of 74 and 50 Ma, the Marion hotspot was influenced by the RTJ and SWIR, respectively, with the

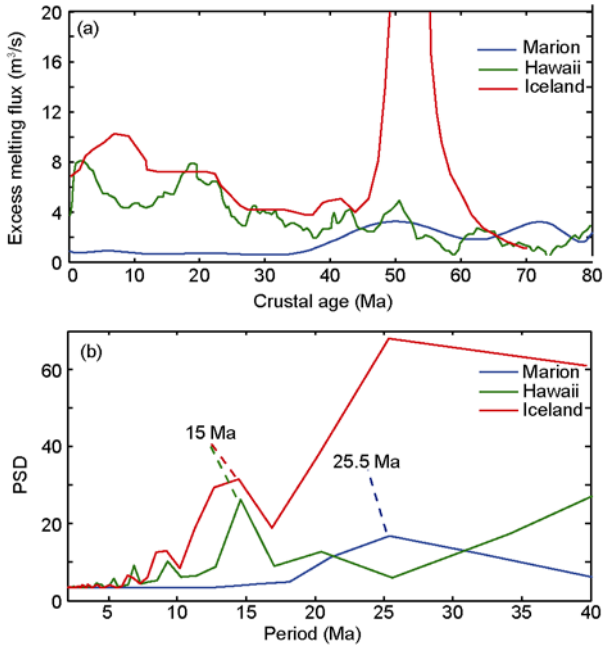

Figure 9 Contrast of excess magmatic flux of hotspots. (a) Excess magmatic fluxes of the Marion hotspot, Hawaii hotspot and Iceland hotspot; (b) power spectral densities (PSD) of excess magmatic flux of the Marion, Hawaii, and Iceland hotspots.

amplitude of activity intensity approximating that of the Hawaii hotspot. In the frequency domain (Figure 9(b)), the quasi-periodicity of the Marion hotspot activity was obviously affected by the distance between the hotspot and the SWIR, and its apparent periodicity of 25.5 Ma corresponded to the two maximum magmatic fluxes at 50 and 74 Ma.

The Hawaii and Iceland hotspots were located in the Pacific and Atlantic, respectively, but had similar respective quasi-periodicities of 16.3 and 15 Ma. Mejelde and Faleide considered accordingly that this similar periodicity represented the large-scale fluctuation of the deep core-mantle boundary and indicated the heat release to the mantle from the Earth's core in a periodic "pulse" with 15 Ma periodicity [5]. The Marion hotspot being far from the Hawaii and Iceland hotspots should be the ideal hotspot to verify this hypothesis. However, the calculated apparent periodicity of the Marion hotspot (25.5 Ma) was significantly longer than that of the Hawaii and Iceland hotspots (about 15 Ma) and was mainly dependent on the distance between the hotspot and the SWIR. Therefore, the case of the Marion hotspot demonstrates that the lithosphere heterogeneity may be an important cause for the quasi-periodicity of hotspot activity.

5.5 Thermal barrier effect of transform faults

Investigation of the RMBA along the SWIR showed that the effect of the Marion hotspot could cross the transform faults of relatively small age offsets like M and ES FZs but was terminated by the ultra-long AB and DII FZs [25]. Accordingly, Georgen et al. [25] believed that the transform faults

had a thermal barrier effect on the hotspot propagation along the spreading center and the blocking effect would be more obvious for longer transform faults. The plate reconstruction in this study shows that the Marion hotspot was always between the DII and IN FZs when the Del Cano Rise was generated by the Marion hotspot with strong magmatism (73.6–42.7 Ma, Figure 5(e)–(h)). In the eastward direction, the propagation of the hotspot along the SWIR (from 65 to 45 Ma) formed a V-shaped bathymetry anomaly. The amplitude of the bathymetry anomaly east of the GA FZ decreased and completely disappeared east of the AII FZ. In the westward direction, the Del Cano Rise did not traverse the DII FZ significantly. This indicates that the DII and AII FZs not only blocked the propagation of the hotspot effects along the spreading ridge but also had a significant thermal barrier effect throughout the whole interaction history of the Marion hotspot and the SWIR. Although the smaller transform faults like IN and GA FZs had a certain thermal barrier effect, they would not have completely blocked the propagation of the hotspot effect along the SWIR.

5.6 Origin of the Crozet hotspot

Owing to the similar distance and tracks of the Conrad and Kerguelen hotspots, the origin and track of the Crozet hotspot have been a topic of debate. Curray et al. [36] inferred that the track of the Crozet hotspot on the Indian plate was from Rajmahal Traps (120 Ma) to Afanasy Nikitin Plateau (70 Ma) through the 85°E Ridge. Curray et al. [36] argued that the Rajmahal Traps is a large igneous province generated at the initiation time of the Crozet hotspot, the 85°E Ridge was the track of the hotspot, while the Afanasy Nikitin Plateau was generated in the process of the hotspot interacting with the India-Antarctica Ridge. However, other geophysical and geochemical evidence does not support this view. On the basis of the reconstruction of a hotspot reference frame (used in this study) and the plate reconstruction of hotspot absolute motion [31, 49], Muller et al. [30, 50] considered that both the 85°E Ridge and Afanasy Nikitin Plateau originated from the Conrad hotspot, which is no longer active. Other researchers believed that the Rajmahal Traps originated from the Kerguelen hotspot. Kent et al. [51] showed that the Crozet hotspot might not have a relationship with the Rajmahal Traps through analysis of Pb and Sr isotopes. From analysis of the Pb isotope, Mahoney et al. [35] considered that there were great differences in the geochemical characters of the Crozet hotspot and the Afanasy Nikitin Plateau and did not support the inference that the Afanasy Nikitin Plateau was created by the Crozet hotspot.

If the 85°E Ridge is excluded, there are no obvious seamount chains on the track of the Crozet hotspot on the Indian plate (90.0–58.6 Ma) and Antarctic plate (58.6–0 Ma), while the SWIR also had geochemical characters different from those of the Crozet hotspot [35]. Even though errors in the hotspot absolute motion and plate reconstruction were considered, there was no track of the seamount chain consistent with the Crozet hotspot motion in the study area. This indicates that the Crozet hotspot had no obvious magmatism for a long period. This phenomenon is similar to many smaller hotspots classified by Courtillot recently [52, 53]. This further suggests that not all hotspots have a noticeable track of a significant seamount chain.

6 Conclusions

Most seamounts in the study region of the Southwest Indian Ocean are related to the Marion hotspot and its interaction with the SWIR. The Del Cano Rise was the result of the interaction of the Marion hotspot with the Rodrigues triple junction and the SWIR as well as the effect of intra-plate volcanism in different phases. The ridge-shaped bathymetry anomaly extending from the Madagascar Plateau to the SWIR is thought to originate from the volcanism of the Marion hotspot penetrating transform faults rather than the track of the hotspot. The propagation of the Marion hotspot effect along the paleo-ridge was restricted by transform faults, and its attenuation correlated to the geometry of transform faults. The magmatic flux of the Marion hotspot was related to the distance between the hotspot and the SWIR. The excess magmatic flux generated was greater when the Marion hotspot approached RTJ and the SWIR than when the hotspot was far away from the SWIR. The quasi-periodicity of the Marion hotspot activity was controlled by its separation distance from the triple junction and the SWIR. The resultant apparent periodicity was significantly longer than the apparent periodicities of the Hawaii and Iceland hotspots.

Many thanks are given to Dr. Daniel Sauter of the French National Center for Scientific Research (CNRS) for providing multi-beam data of the Southwest Indian Ridge, and Dr. Zhao Lihong of the Shandong University of Science and Technology for providing the hotspot trace modeling program. This study benefited greatly from discussions with Dr. Sun Zhen of the South China Sea Institute of Oceanology, Chinese Academy of Sciences, Dr. Zhu Jian of the Woods Hole Oceanographic Institution, Dr. Wang Tingting of Peking University, Dr. Jennifer Georgen of Old Dominion University, USA, and Dr. Wu Zhaocai, Dr. Shen Zhongyan and Dr. Yang Chunguo of the Second Institute of Oceanography, State Oceanic Administration. Most figures used in this study were drawn with GMT (Wessel & Smith [53]). This work was supported by SOA Funds for Young Scientists (Grant Nos. 1084-10) and Special Funding for the Basic Scientific Research (Grant Nos. JG0706 and JG0716).

1 Wessel P. Sizes and ages of seamounts using remote sensing: Implications for intraplate volcanism. Science, 1997, 277: 802–805
2 Morgan W. Rodriguez, Darwin, Amsterdam, a second type of hotspot island. J Geophys Res, 1978, 83: 5355–5360
3 Escartín J, Cannat M, Pouliquen G, et al. Crustal thickness of V-shaped ridges south of the Azores: Interaction of the Mid-Atlantic Ridge (36°–39°N) and the Azores hot spot. J Geophys Res, 2001, 106: 21719–21735
4 Van Ark E, Lin J. Time variation in igneous volume flux of the Ha-

waii-Emperor hot spot seamount chain. J Geophys Res, 2004, 109: B11401, doi: 10.1029/2003JB002949
5 Mjelde R, Faleide J. Variation of Icelandic and Hawaiian magmatism: Evidence for co-pulsation of mantle plumes? Marine Geophys Res, 2009, 30: 61–72
6 Ito G, Lin J. Oceanic spreading center-hotspot interactions: Constraints from along-isochron bathymetric and gravity anomalies. Geology, 1995, 23: 657–660
7 Maia M, Goslin J, Gente P. Evolution of the accretion processes along the Mid-Atlantic Ridge north of the Azores since 5.5 Ma: An insight into the interactions between the ridge and the plume. Geochem Geophys Geosyst, 2007, 8: Q03013, doi: 10.1029/2006GC001318
8 Vidal V, Bonneville A. Variations of the Hawaiian hot spot activity revealed by variations in the magma production rate. J Geophys Res, 2004, 109: B03104, doi: 10.1029/2003JB002559
9 Adam C, Vidal V, Escartín J. 80-Myr history of buoyancy and volcanic fluxes along the trails of the Walvis and St. Helena hotspots (South Atlantic). Earth Planet Sci Lett, 2007, 261: 432–442
10 Jokat W, Ritzmann O, Schmidt-Aursch M C, et al. Geophysical evidence for reduced melt production on the Arctic ultraslow Gakkel mid-ocean ridge. Nature, 2003, 423: 962–965
11 Gente P, Dyment J, Maia M, et al. Interaction between the Mid-Atlantic Ridge and the Azores hot spot during the last 85 Myr: Emplacement and rifting of the hot spot-derived plateaus. Geochem Geophys Geosyst, 2003, 4: 8514, doi: 10.1029/2003GC000527
12 Dick H J B, Lin J, Schouten H. An ultraslow-spreading class of ocean ridge. Nature, 2003, 426: 405–412
13 Tao C, Lin J, Guo S, et al. First discovery and investigation of a high temperature hydrothermal vent field on the ultraslow spreading Southwest Indian Ridge. EOS Trans AGU Fall Meet Suppl Abstract, 2007. T52B-07
14 Goslin J, Patriat P. Absolute and relative plate motions and hypotheses on the origin of five aseismic ridges in the Indian Ocean. Tectonophys, 1983, 101: 221–244
15 Coffin M F, Eldholm O. Large Igneous Provinces: Crustal structure, dimensions, and external consequences. Rev Geophys, 1994, 32: 1–36
16 Sinha M C, Louden K E, Parsons B. The crustal structure of the Madagascar Ridge. Geophys J Roy Astro Soc, 1981, 66: 351–377
17 Smith W H F, Sandwell D T. Global sea floor topography from satellite altimetry and ship depth soundings. Science, 1997, 277: 1956–1962
18 Müller R D, Sdrolias M, Gaina C, et al. Age, spreading rates, and spreading asymmetry of the world's ocean crust. Geochem Geophys Geosyst, 2008, 9: Q04006, doi: 10.1029/2007GC001743
19 Patriat P, Segoufin J. Reconstruction of the central Indian Ocean. Tectonophys, 1988, 155: 211–234
20 Cannat M, Rommevaux-Jestin C, Sauter D, et al. Formation of the axial relief at the very slow spreading Southwest Indian Ridge (49° to 69°E). J Geophys Res, 1999, 104: 21825–21843
21 Meyzen C M, Ludden J N, Humler E, et al. New insights into the origin and distribution of the DUPAL isotope anomaly in the Indian Ocean mantle from MORB of the Southwest Indian Ridge. Geochem Geophys Geosyst, 2005, 6: Q11K11, doi: 10.1029/2005GC000979
22 Font L, Murton B J, Roberts S, et al. Variations in melt productivity and melting conditions along SWIR (70°E–49°E): Evidence from olivine-hosted and plagioclase-hosted melt inclusions. J Petrol, 2007, 48: 1471–1494
23 Mendel V, Sauter D, Rommevaux-Jestin C, et al. Magmatic-tectonic cyclicity at the ultra-slow spreading Southwest Indian Ridge: Evidence from variations of axial volcanic ridge morphology and abyssal hills pattern. Geochem Geophys Geosyst, 2003, 4: 9102, doi: 10.1029/ 2002GC000417
24 Sauter D, Patriat P, Rommevaux-Jestin C, et al. The Southwest Indian Ridge between 49°15'E and 57°E: Focused accretion and magma redistribution. Earth Planet Sci Lett, 2001, 192: 303–317
25 Georgen J E, Lin J, Dick H J B. Evidence from gravity anomalies for interactions of the Marion and Bouvet hotspots with the Southwest Indian Ridge: Effects of transform offsets. Earth Planet Sci Lett, 2001, 187: 283–300
26 Muller M R, Minshull T A, White R S. Crustal structure of the Southwest Indian Ridge at the Atlantis II Fracture Zone. J Geophys Res, 2000, 105: 25809–25828
27 Muller M R, Minshull T A, White R S. Segmentation and melt supply at the Southwest Indian Ridge. Geology, 1999, 27: 867–870
28 Minshull T A, Muller M R, White R S. Crustal structure of the Southwest Indian Ridge at 66°E: Seismic constraints. Geophys J Int, 2006, 166: 135–147
29 Goslin J, Segoufin J, Schlich R, et al. Submarine topography and shallow structure of the Madagascar Ridge, western Indian Ocean. Geol Soc Am Bull, 1980, 91: 741–753
30 Duncan R A, Richards M A. Hotspots, mantle plumes, flood basalts, and true polar wander. Rev Geophys, 1991, 29: 31–50
31 Muller RD, Royer J Y, Lawver L A. Revised plate motions relative to the hotspots from combined Atlantic and Indian Ocean hotspot tracks. Geology, 1993, 21: 275–278
32 Storey M, Mahoney J, Saunders A D, et al. Timing of hot spot-related volcanism and the breakup of Madagascar and India. Science, 1995, 267: 852–855
33 Goslin J, Diament M. Mechanical and thermal isostatic response of the Del Cano Rise and Crozet Bank (southern Indian Ocean) from altimetry data. Earth Planet Sci Lett, 1987, 84: 285–294
34 Recq M, Goslin J, Charvis P, et al. Small-scale crustal variability within an intraplate structure: the Crozet Bank (southern Indian Ocean). Geophys J Int, 1998, 134: 145–156
35 Mahoney J J, White W M, Upton B G J, et al. Beyond EM-1: Lavas from Afanasy-Nikitin Rise and the Crozet Archipelago, Indian Ocean. Geology, 1996, 24: 615–618
36 Curray J R, Munasinghe T. Origin of the Rajmahal Traps and the 85° E Ridge: Preliminary reconstructions of the trace of the Crozet hotspot. Geology, 1991, 19: 1237–1240
37 Divins D L. Thickness of sedimentary cover in the Eastern Pacific Ocean. In: Udintsev G B, ed, International Geological-Geophysical Atlas of the Pacific Ocean. 2003. 120, 126, 127, 130
38 McKenzie D. Some remarks on the development of sedimentary basins. Earth Planet Sci Lett, 1978, 40: 25–32
39 Parsons B, Sclater J. An analysis of the variation of ocean floor bathymetry and heat flow with age. J Geophys Res, 1977, 82: 802–827
40 Stein C A, Stein S. A model for the global variation in oceanic depth and heat flow with lithospheric age. Nature, 1992, 359: 123–129
41 Crough S T. The correction for sediment loading on the seafloor. J Geophys Res, 1983, 88: 6449–6454
42 Sauter D, Cannat M, Meyzen C, et al. Propagation of a melting anomaly along the ultraslow Southwest Indian Ridge between 46°E and 52°20′E: Interaction with the Crozet hotspot? Geophys J Int, 2009, 179: 687–699
43 Tucholke B E, Lin J. A geological model for the structure of ridge segments in slow spreading ocean crust. J Geophys Res, 1994, 99: 11937–11958
44 DeMets C, Gordon R, Argus D, et al. Current plate motions. Geophys J Int, 1990, 101: 425–478
45 White R S. Melt production rates in mantle plumes. Phil Trans Roy Soc Lond Ser A-Phys Engineering Sci, 1993, 342: 137–153
46 Wessel P. An empirical method for optimal robust regional-residual separation of geophysical data. Math Geol, 1998, 30: 391–408
47 O'Neill C, Muller D, Steinberger B. Geodynamic implications of moving Indian Ocean hotspots. Earth Planet Sci Lett, 2003, 215: 151–168
48 Douglass J, Schilling J G, Kingsley R H, et al. Influence of the discovery and Shona mantle plumes on the Southern Mid-Atlantic Ridge: Rare Earth evidence. Geophys Res Lett, 1995, 22: 2893–2896
49 Muller R D, Roest W R, Royer J Y. Asymmetric sea-floor spreading caused by ridge-plume interactions. Nature, 1998, 396: 455–459
50 Morgan W J. Deep mantle convection plumes and plate motions. AAPG Bull, 1972, 56: 203–213
51 Kent W, Saunders A D, Kempton P D, et al. Rajmahal basalts, eastern India: Mantle sources and melt distribution at a volcanic rifted margin. AGU Geophys Monogr, 1997, 100: 145–182
52 Courtillot V, Davaille A, Besse J, et al. Three distinct types of hotspots in the Earth's mantle. Earth Planet Sci Lett, 2003, 205: 295–308
53 Wessel P, Smith W H F. New version of the Generic Mapping Tools released. EOS Trans AGU, 1995, 76: 329